The MAP kinase-activated protein kinase 2 (MK2) contributes to the Shiga toxin-induced inflammatory response

Jose B. Saenz, **Jinmei Li**, and **David B. Haslam**
Department of Pediatrics, Washington University School of Medicine 660 S. Euclid Avenue St. Louis, MO 63110, USA

Summary

Infection with Shiga toxin (STx)-producing bacteria can progress to a toxemic, extraintestinal injury cascade known as hemolytic uremic syndrome (HUS), the leading cause of acute renal failure in children. Mounting evidence suggests that STx activates stress response pathways in susceptible cells and has implicated the p38 mitogen-activated protein kinase (MAPK) pathway. More importantly, some of the pathology associated with HUS is believed to be a result of a STx-induced inflammatory response. From a siRNA screen of the human kinome adapted to a high-throughput format, we found that knock-down of the MAPK-activated protein kinase 2 (MK2), a downstream target of the p38 MAPK, protected against Shiga toxicity. Further characterization of the *in vitro* role of MK2 revealed that STx activates the p38-MK2 stress response pathway in both p38- and MK2-dependent manners in two distinct cell lines. MK2 activation was specific to damage to the ribosome by an enzymatically active toxin and did not result from translational inhibition per se. Genetic and chemical inhibition of MK2 significantly decreased the inflammatory response to STx. These findings suggest that MK2 inhibition might play a valuable role in decreasing the immuopathological component of STx-mediated disease.

Introduction

Bacterial exotoxins are critical components of bacterial pathogenesis and constitute potential vehicles for bioterrorism. Among the most studied of the bacterial toxins are members of the AB family, including the bacterial toxins Shiga toxin (STx) and the plant toxin ricin. These toxins are characterized by their bipartite structure, consisting of a pentameric, receptor-binding B moiety that is non-covalently linked to a catalytic A subunit. Following a unique retrograde trafficking pathway that facilitates toxin access to the cytosol (Yu and Haslam, 2005; Falguieres *et al.*, 2001; Falnes and Sandvig, 2000; Simpson *et al.*, 1999), these toxins shut off host protein synthesis by inactivating the ribosome through cleavage of a single adenine residue in the 28S rRNA (Obrig *et al.*, 1987; Endo and Tsurugi, 1986; Reisbig *et al.*, 1981).

STx was initially identified in *Shigella dysenteriae* type I, though it is now commonly associated with strains of STx-producing *Escherichia coli* (STEC), among which *E. coli* O157:H7 has become the most clinically relevant. In a subset of patients, gastrointestinal infection with STEC may progress to extraintestinal injury, leading to hemorrhagic colitis and hemolytic uremic syndrome (HUS). This toxemic syndrome is clinically defined by renal failure, thrombocytopenia, and hemolytic anemia, and it remains the leading cause of acute renal failure in children (Griffin and Tauxe, 1991; Karmali, 1989). Extraintestinal complications of HUS correlate with circulating levels of STx, though the mechanism of

Correspondence: haslam@kids.wustl.edu Tel. (314) 286-2888; Fax (314) 286-2895.

STx-induced pathology in HUS remains unclear. One of the hallmarks of HUS is the development of thrombotic lesions within the intestinal and renal microvasculature that accounts for the associated hemorrhagic colitis, hemolytic anemia, and renal failure (Proulx *et al.*, 2001). Though some evidence would suggest a direct role for STx in the thrombotic microangiopathy associated with HUS (Louise and Obrig, 1992; Obrig *et al.*, 1988), various lines of evidence support the view that much of the systemic and focal pathology of HUS is immune-mediated (Te Loo *et al.*, 2006; van Setten *et al.*, 1997; Ramegowda and Tesh, 1996; Kaye *et al.*, 1993; van de Kar *et al.*, 1992).

In conjunction with the mounting evidence suggesting an inflammatory contribution to HUS pathology, various cellular stress pathways have been implicated. Perhaps the most studied are members of the mitogen activated protein kinase (MAPK) family. MAPKs are signal-transducing enzymes involved in a variety of regulatory roles in eukaryotes, including inflammation, differentiation, and apoptosis (Ono and Han, 2000). The p38 MAPK (p38) plays a critical role in the response to various stresses, such as UV radiation, cytokines, and toxic stress (Zarubin and Han, 2005). In the context of STx-mediated damage, numerous studies have clearly defined the role of p38 in inciting inflammatory cytokine release from toxin-treated cells (Stone *et al.*, 2008; Foster and Tesh, 2002). One study, for example, showed that sequence-specific damage to 28S rRNA by STx stimulated a ribotoxic stress response that resulted in p38 activation (Smith *et al.*, 2003).

Though the mechanisms behind STx activation of these signaling cascades remain unclear, a critical component is the function of kinases in propagating the stress signal and initiating a cellular response. As a result, kinases are tempting therapeutic targets for limiting STx-mediated cellular injury. For example, inhibition of p38 activation decreased cytokine release following exposure of macrophages to STx (Cherla *et al.*, 2006). However, p38 inhibition may have limited therapeutic potential, given the ability of p38 to activate various downstream kinases involved in diverse cellular functions. Indeed, mice deficient in p38 are not viable post-natally (Allen *et al.*, 2000; Mudgett *et al.*, 2000; Tamura *et al.*, 2000), and in human clinical trials p38 inhibition has been met with unanticipated side effects (Dominguez *et al.*, 2005). Moreover, inhibition of p38 kinase activity by overexpression of dominant negative p38 isoforms (Somwar *et al.*, 2002) or by treatment with chemical inhibitors (Henry *et al.*, 1998) has made probing of specific p38-dependent signaling pathways particularly difficult. Effectors downstream of p38 might therefore be more specific and functionally relevant to the inflammatory signals induced in response to STx (Gaestel *et al.*, 2009).

The mitogen-activated protein kinase-activated protein kinase 2 (MK2) has been recently shown to contribute to the inflammatory response (Kotlyarov *et al.*, 1999). MK2 is a member of the MK subfamily of calcium/calmodulin-dependent kinases that was originally identified as an *in vivo* substrate of p38 (Gaestel, 2006). Activation of MK2 by p38 results primarily in the subsequent phosphorylation of its two main substrates, heat shock protein 27 (Hsp27) and tristetraprolin (TTP). Despite evidence demonstrating that STx elicits a p38-dependent stress response *in vitro* (Smith *et al.*, 2003) and that MK2 has been implicated in an *in vivo* inflammatory response to LPS (Kotlyarov *et al.*, 1999), the role of MK2 in STx-mediated toxicity has yet to be explored. From a high-throughput siRNA screen of the human kinome, knock-down of MK2 was found to protect against Shiga toxicity. We present evidence demonstrating that STx activates MK2 *in vitro* in a p38-dependent manner and that inhibition of MK2 decreases the STx-induced inflammatory cytokine response.

Results

Knock-down of MK2 protects against Shiga toxicity

Various approaches have been employed to study the biological mechanisms underlying toxin-induced cell death. Of particular interest, high-throughput screens of small molecules have been developed to target varying aspects of bacterial toxin pathogenesis (Saenz *et al.*, 2007; Hung *et al.*, 2005; Carey *et al.*, 2004). While small molecule compounds are amenable to high-throughput screening and allow for the reversible manipulation of cellular processes, the rate-limiting step in these studies is the identification of the compound's target (Saenz *et al.*, 2009).

As a result, we adapted an inherently target-based approach to specifically screen for kinases involved in Shiga toxicity. An siRNA library targeting 646 human kinase and kinase-associated genes (Supplementary Experimental Procedures) was optimized to a high-throughput format and screened for kinases essential to Shiga toxicity in HeLa cells. A HeLa cell line (HeLa-Fluc) that constitutively expressed luciferase (Gross and Piwnica-Worms, 2005), where light expression served as a translational readout, was transfected with a duplex of each of 646 siRNAs targeting the human kinome (Experimental Procedures) prior to treatment with STx (1 ng/mL) for 24 h. Each plate incorporated a series of controls to assess the screen for siRNA transfection efficiency and discriminatory ability (Supplementary Fig. 2). We considered a hit any kinase knock-down that, in the presence of STx, maintained light levels at least 3 standard deviations above mock-transfected, STx-treated controls on replicate plates. Of six kinase hits identified, the mitogen-activated protein kinase-activated protein kinase 2 (MK2) revealed the strongest protective effect (Fig. 1), and its role in STx-induced cytotoxicity was investigated.

STx activates MK2 in vitro

MK2 is a member of the calcium/calmodulin-dependent superfamily of kinases functioning downstream of the p38 MAP kinase (Gaestel, 2006). Activation of MK2 by p38 results in the subsequent phosphorylation by MK2 of its two main substrates, Hsp27 and tristetraprolin (TTP). Hsp27 phosphorylation has been demonstrated to be completely dependent on the kinase activity of MK2 (Anderson *et al.*, 2005), and we therefore used Hsp27 phosphorylation as an indicator of MK2 activation. Since the p38 MAPK pathway has been shown to play a critical role in the response to various stresses, including UV radiation, cytokines, and toxic stress, we assessed STx activation of MK2 in HeLa cells by monitoring Hsp27 phosphorylation. Treatment with STx resulted in activation of MK2 in both a time- and dose-dependent manner. As early as 60 min following exposure to STx, phosphorylation of MK2 and its downstream target, Hsp27, were observed (Fig. 2A). Similarly, higher levels of phosphorylated MK2 and Hsp27 were observed with increasing STx concentrations (Fig. 2B). Time- and dose-dependent phosphorylation of the p38 MAPK mirrored that of MK2, suggesting activation of the p38-MK2 pathway (Fig. 2). In addition, we confirmed that MK2 activation was not the result of a lipopolysacchride (LPS) contamination of the toxin preparation, as heat-inactivated STx (HI-STx) failed to activate MK2 (Fig. 2C).

Some studies have suggested that STxB binding to its receptor can stimulate signal transduction cascades following activation of membrane-localized kinases, such as Syk (Lauvrak *et al.*, 2006) and Yes (Katagiri *et al.*, 1999), and that these effects were independent of the toxin's effect on ribosome function. We found, however, that exposure of HeLa cells to the STxB subunit alone did not result in Hsp27 phosphorylation (Fig. 2C), implying that engagement of the STx receptor, Gb3, by the receptor-binding B subunit is insufficient for MK2 activation and that STx's catalytic activity is necessary for induction of

this pathway. Phosphorylation of MK2 in the presence of STx thus appears to be specific to an enzymatically active toxin.

Activation of MK2 is p38-dependent

To assess the role of p38 on STx-induced MK2 activation, we treated HeLa cells with the p38-selective chemical inhibitor, SB202190, prior to STx exposure. As expected, pretreatment with SB202190 blocked Hsp27 phosphorylation, indicating that STx specifically activates MK2 through p38 and not through another stress activation pathway (Fig. 2C). Moreover, pretreatment with other p38 inhibitors (SB 203580, p38 inhibitor III) showed a similar effect, while pretreatment with the JNK inhibitor (SP 600125) showed no decrease in MK2 activation in the presence of STx (Fig. 3). Taken together, these results indicate that STx-induced activation of MK2 is dependent on its upstream MAP kinase, p38.

While we could confirm that STx stimulated the p38 MAPK pathway in HeLa cells, we sought to validate these findings in a more physiologically relevant cell line. Much of the *in vivo* systemic pathology resulting from infection with STx-producing bacteria is related to the effects of circulating levels of STx on microvasculature (Tarr *et al.*, 2005). STx-mediated endothelial cytotoxicity is believed to contribute to the thrombotic microangiopathy of HUS, and exposure of endothelial cells to STx has been shown to induce thrombotic changes to the endothelial cell surface, further contributing to the pro-coagulant state observed in HUS (Morigi *et al.*, 2001). We investigated the *in vitro* effects of STx on human microvascular endothelial cells (HMVEC). As with HeLa cells, STx treatment of HMVEC stimulated MK2 activity in a time- and dose-dependent manner (Figs. 2A-B), and MK2 activation was shown to be p38-dependent (Fig. 3).

In these experiments we measured cellular responses to STx1 (Fig. 2) and STx2 (Fig. 3), though we have found that HMVEC cells consistently showed similar sensitivity to both STx subgroups in terms of p38 activation (data not shown). While both subgroups differ in their toxicity in mice (Lindgren *et al.*, 1994;Paros *et al.*, 1993;Samuel *et al.*, 1990), they share indistinguishable toxicity in our cultured HMVEC (not shown) and HeLa cells (Supplementary Fig. 5B), consistent with similar observations in Vero cells (Tesh *et al.*, 1993). However, epidemiological evidence suggests that *stx2*-producing enterohemorrhagic *E. coli* (EHEC) O157:H7 strains are more frequently associated with HUS than are *stx1*-producing strains (Ostroff *et al.*, 1989;Scotland *et al.*, 1987). We therefore found it relevant to study both STx subgroups in the context of p38-MK2 activation.

STx activation of the p38-MK2 pathway requires MK2 enzymatic activity

Activation of the p38-MK2 pathway by STx was equally found to be dependent on MK2 catalytic activity. Overexpression of a catalytically inactive adenoviral construct (MK2-DN) in HeLa cells eliminated STx1-induced Hsp27 phosphorylation compared to cells overexpressing wild-type MK2 (MK2-WT) or control vector (pAd-Luc; Fig. 4A). To validate this finding and further confirm the role of catalytically active MK2 in the response to STx, pretreatment of endothelial cells with a recently identified inhibitor of MK2, PHA-781089, blocked STx1-induced Hsp27 phosphorylation. This compound, at a dose of 20 μM, has been previously shown to inhibit Hsp27 phosphorylation of LPS-treated U937 macrophage cells. In addition, its selectivity for MK2 has been validated in cell-free and cell-based systems (Anderson *et al.*, 2005). We found a similar dose response of PHA-781089 against Hsp27 phosphorylation in STx1-treated HeLa cells (Supplementary Figure 5A). Treatment of HMVEC with 20 μM PHA-781089 resulted in undetectable levels of phosphorylated Hsp27, even after 4 h of STx treatment, while vehicle-treated controls demonstrated MK2 activity beginning at 60 mins (Fig. 4B). This effect was not the result of the MK2 inhibitor on STx transport, as treatment of HeLa cells with PHA-781089 showed

no effects on STxB-488 transport to the Golgi (Supplementary Fig. 5C). Previous studies had demonstrated that inhibition of p38 blocked STx transport and signaling (Skanland *et al.*, 2009;Walchli *et al.*, 2008), though our studies found no effects of MK2 inhibition on STx transport to the Golgi in HeLa cells over the time course studied. Our findings suggest that STx stimulates the p38-MK2 pathway in two distinct human cell lines and that activation of the p38-MK2 pathway may contribute to the endothelial cellular stress response to STx *in vivo*.

MK2 activation by STx is dependent on toxin adherence and intracellular transport

STx, like the plant toxin ricin, follows a retrograde trafficking pathway to reach its intracellular target. Following endocytosis into an early endosome, it is believed that these toxins hijack host trafficking mechanisms in order to bypass lysosomal degradation (Wilcke *et al.*, 2000) and coordinate their rerouting to the ER via the Golgi (Saenz *et al.*, 2007). The toxins are then retrotranslocated across the ER membrane in order to access the cytosol, where they can inhibit protein synthesis by directly damaging the ribosome (Yu and Haslam, 2005; Yu *et al.*, 2000; Simpson *et al.*, 1999). To test whether MK2 activation relied on STx transport to the cytosol, HMVEC were initially incubated with P1 glycoprotein, a ligand of the Gb3 receptor. As STx is known to induce its uptake following binding to the glycosphingolipid Gb3 (Takenouchi *et al.*, 2004), we would expect that co-incubation of STx1 with the P1 glycoprotein would prevent toxin endocytosis. Indeed, the P1 glycoprotein reduced cell surface-associated STx1 and protected against STx1-mediated inhibition of protein synthesis (Supplementary Figs. 6A-B). More importantly, the P1 glycoprotein was able to protect against STx-induced p38 and Hsp27 phosphorylation, suggesting that STx must be internalized to stimulate the p38-MK2 pathway (Fig. 5A). Similarly, treatment of HMVEC with Golgicide A (GCA), a potent inhibitor of Shiga toxicity that arrests STx transport at the early endosome (Saenz *et al.*, 2009), was shown to also prevent STx-induced p38 and Hsp27 phosphorylation. In contrast, GCA had no effect on anisomycin, an established p38 agonist (Wang *et al.*, 2005) that does not rely on intracellular transport and that rapidly equilibrates in the cytosol. If we equally consider that treatment with STxB alone did not activate MK2 (Fig. 2C), these results would collectively suggest that transport of catalytically active STx to the cytosol is required to activate the p38-MK2 pathway.

MK2 activation relies on damage to the ribosome

Following entry into the cytosol, STx and ricin inhibit protein synthesis through sequence-specific RNA damage to the α-sarcin loop in the 28S rRNA (Iordanov *et al.*, 1997). Both toxins consist of an enzymatic A subunit that has RNA *N*-glycohydrolase activity and depurinates a single adenine residue at position 4324 of the 28S rRNA. Given that MK2 activation relied on enzymatically active STx (Fig. 2C), we examined the possibility that MK2 activation was the result of ribosomal damage and not simply a stress response due to translational inhibition. To test this, HMVEC were treated with various inhibitors of protein synthesis acting through distinct mechanisms, and activation of the p38-MK2 pathway was assessed . As expected, STx and ricin treatments both stimulated p38 and Hsp27 phosphorylation (Fig. 5B). In addition, both clinically relevant STx subgroups, STx1 and STx2, stimulated a similar response. These subgroups show approximately 60% similarity in the A subunits at the amino acid level (Proulx *et al.*, 2001) and share a common enzymatic mechanism. The bacterial exotoxins diphtheria toxin (DT) and *Pseudomonas* exotoxin A (PE), however, were unable to stimulate the p38-MK2 pathway at concentrations that have been previously shown to inhibit protein synthesis in HeLa cells (Zhao and Haslam, 2005). Both toxins inhibit protein synthesis by catalyzing the ADP ribosylation of elongation factor 2 (Deng and Barbieri, 2008; Yates and Merrill, 2004). Similarly, the aminonucleoside antibiotic puromycin, which arrests translation by causing a premature release of the nascent peptide (Pestka, 1971), also failed to activate the p38-MK2 pathway, while cycloheximide,

which prevents ribosomal translocation during translational elongation (Pestka, 1971), weakly activated it. These findings are consistent with activation of the p38-MK2 pathway following specific damage to the ribosome and not translational inhibition per se.

MK2 inhibition decreases the inflammatory response to STx

MK2 has been implicated in a variety of stress responses, most notably inflammation (Kotlyarov *et al.*, 1999), though no studies have directly assessed MK2's role in the context of the STx-induced inflammatory response. Multiple studies have lent an immmunological perspective to the pathology of HUS (Te Loo *et al.*, 2006; van Setten *et al.*, 1997; Ramegowda and Tesh, 1996). Given the activation of the p38-MK2 stress response pathway by STx and the contribution of this pathway to inflammation, we assessed the role of MK2 in generating an inflammatory response to STx. HeLa cells were transduced with adenoviral constructs expressing wild-type MK2 (MK2-WT) or a catalytically inactive MK2 (MK2-DN). Expression of these constructs was validated (Supplementary Fig. 7) and exhibited the expected effects on STx1-induced MK2 activation (Fig. 4A). MK2-DN overexpression significantly reduced mRNA levels of the inflammatory cytokines IL-6 and TNFα compared to cells overexpressing MK2-WT, as assessed by quantitative PCR (qPCR; Figs. 6A-B). This suggests that catalytically active MK2 is required for the STx1-induced expression of the inflammatory markers IL-6 and TNFα.

To further confirm that MK2 inhibition reduced the cytokine response to STx1, HeLa cells were pretreated with DMSO, an MK2 inhibitor, or a p38 inhibitor prior to a 6-h exposure to STx1. Chemical inhibition of MK2 significantly reduced IL-6 and TNFα mRNA levels (Figs. 6C-D), consistent with overexpression of catalytically inactive MK2 (Figs. 6A-B). Similarly, chemical inhibition of p38, the kinase upstream of MK2, also significantly reduced the levels of these general inflammatory cytokines (Figs. 6C-D). These results collectively show that genetic and chemical inhibition of MK2 activity significantly reduces the inflammatory response to STx1. Chemical inhibition of MK2 thus presents a unique opportunity for targeting the immunopathological response to STx *in vivo*.

Discussion

In an effort to identify kinases involved in Shiga toxicity, we developed and adapted a siRNA screen targeting the human kinome to identify kinases essential to STx-induced cytotoxicity. Of the 646 kinases tested, six were identified as protective, with MK2 exhibiting the greatest protection. Compared to previous high-throughput screens aimed at identifying small molecule inhibitors of microbial toxicity (Saenz *et al.*, 2009; Saenz *et al.*, 2007; Hung *et al.*, 2005; Carey *et al.*, 2004), the siRNA approach represents an inherently target-based approach that is not hampered by potential intracellular "off-target" effects of small molecules.

While previous screens (Saenz *et al.*, 2009; Saenz *et al.*, 2007) focused on inhibitors of toxin trafficking and monitored Shiga toxicity over a shorter time period (~ 4-6 h), the siRNA screen relied on a 24-h exposure to STx due to the relatively long half-life of the Fluc translational reporter (Supplementary Fig. 3). As a result, we would expect that, following a longer exposure to STx, knock-down of kinases involved in STx transport as well as those involved in STx-induced cell death would show up as protective. Indeed, knock-down of MK2 exhibited strong protection against Shiga toxicity in our screen. A subsequent assessment of cell viability by Alamar Blue staining revealed that wells transfected with MK2 siRNA showed relatively higher cell viability (Supplementary Fig. 2), which may have accounted for the protective effects observed. Knock-down of MK2 by siRNA resulted in reduced levels of MK2 protein but did not correlate with reduced Hsp27 phosphorylation following exposure to STx1 (not shown). Given the ability of the MK2 inhibitor to

significantly reduce STx1-mediated Hsp27 phosphorylation, this discrepancy may be explained by residual MK2 levels following siRNA-mediated knock-down that were able to phosphorylate Hsp27. Indeed, a recent study concluded that signaling downstream of MK2 depends on the relative percent of MK2 phosphorylation and not on the absolute amount of phospho-protein (Janes *et al.*, 2008). siRNA-mediated knock-down of MK2 desensitized the pathway of MK2 activation such that only very strong activation could lead to a productive (and detectable) output from endogenous MK2. This may explain the ability of MK2 to phosphorylate Hsp27, despite reduced MK2 levels, in the presence of STx. Chemical inhibition of MK2 using PHA-781089 inhibits catalytic activity of endogenous MK2 and likely desensitizes this pathway regardless of the level of STx activation.

The central role of the p38 MAPK in propagating various cellular stress responses (Ono and Han, 2000) has made specific inhibition of p38-dependent signaling pathways particularly difficult. MK2 thus appears as a tempting target, given that it functions downstream of p38 on a smaller set of substrates (Gaestel, 2006). More importantly, MK2 has been implicated in the inflammatory response in a lipopolysaccharide (LPS) mouse model (Kotlyarov *et al.*, 1999): MK2-deficient mice showed decreased TNFα and IL-6 levels and increased survival to LPS-induced shock. In an experimental asthma model, MK2 was found to be essential to Th2-type inflammation through sustained NF-κB activation (Gorska *et al.*, 2007). Most recently, selective MK2 inhibitors have been developed for the treatment of rheumatoid arthritis and other inflammatory conditions mediated by TNFα (Anderson *et al.*, 2007). The contribution of the inflammatory response in HUS remains debated, though several lines of evidence would suggest that some of the systemic pathology, namely the development of thrombotic lesions within the renal microvasculature, could be an immunopathological phenomenon (Ramegowda and Tesh, 1996; Harel *et al.*, 1993; Kaye *et al.*, 1993). Our studies suggest that catalytically active STx activates MK2 as a result of ribosomal damage, implicating MK2 in the STx ribotoxic stress response.

Biochemical evidence suggests that MK2 contributes to the stability of IL-6 and TNFα mRNA through the downstream phosphorylation of TTP in a process that involves AU-rich elements (ARE) in the 3' non-coding regions of these mRNAs (Sun *et al.*, 2007; Stoecklin *et al.*, 2004; Neininger *et al.*, 2002; Carballo *et al.*, 2001; Mahtani *et al.*, 2001): phosphorylation of TTP by MK2 results in TTP sequestration and prevents TTP from directing degradation of these mRNAs. In our studies, MK2 inhibition by genetic and chemical means diminished the acute inflammatory response in STx-treated HeLa cells. Overexpression of catalytically inactive MK2 significantly decreased the mRNA levels of IL-6 and TNFα, and chemical inhibition of MK2 mirrored these effects.

Interestingly, HMVEC under the same tissue culture conditions did not exhibit the cytokine response that was observed in HeLa cells, despite demonstrating STx-dependent activation of the p38-MK2 pathway *in vitro*. Our studies utilized HMVEC of dermal origin, whose sensitivity to STx is similar to that of Vero cells (Pijpers *et al.*, 2001). Certain human microvascular endothelial cell lines have been shown to mount a STx-dependent cytokine response *in vitro* (Guessous *et al.*, 2005; Stricklett *et al.*, 2005), though these responses appear to be cell origin-dependent (Obrig *et al.*, 1993) and require pre-sensitization with inflammatory cytokines. Nonetheless, the observed cytokine response in HeLa cells, though relatively lower than the STx-induced cytokine response in macrophages, for example (Ramegowda and Tesh, 1996), could be crucial to establishing a local inflammatory milieu *in vivo*. In particular, decreased *in vitro* levels of the general inflammatory markers TNFα and IL-6 in MK2-inhibited cells is consistent with decreased cytokine expression in MK2-deficient mice (Kotlyarov *et al.*, 1999) and could translate to decreased immunopathology following exposure to STx. Inhibition of MK2 thus presents a viable therapeutic option in mitigating the toxemic effects of STx-mediated disease.

Experimental Procedures

Reagents and Antibodies

Shiga toxin 1 (STx1) and 2 (STx2) were kindly provided by Anne Kane (Tufts University) and diluted to 0.5 mg/mL in PBS (pH 7.4). Aliquots were frozen at −80°C until further use. Ricin, *Pseudomonas* exotoxin A, and diphtheria toxin were purchased from Sigma. The B subunit of STx1 (STxB) was purified and fluorescently tagged as previously described (Saenz *et al.*, 2007). SB202190, SB203580, SP600125, anisomycin, puromycin, cycloheximide, and DMSO were purchased from Sigma, p38 inhibitor III from Calbiochem, and Golgicide A from ChemDiv. The MK2 inhibitor, PHA-781089, was obtained from Pfizer through a Material Transfer Agreement. All chemical inhibitors were diluted to 10 mM in DMSO and stored at −20°C until further use. All antibodies used for Western blotting were purchased from Cell Signaling Technology, Inc. Dulbecco's modified Eagle's medium (DMEM), streptomycin, and penicillin were from Mediatech, and fetal bovine serum (FBS) was from Hyclone. Protease inhibitor cocktail was from Roche.

Cell culture

HeLa cells were obtained from the Tissue Culture Support Center (Washington University) and maintained at 37°C and 5% CO_2 in DMEM supplemented with 10% FBS and 0.1% penicillin/streptomycin. HeLa-Fluc cells were kindly provided by David Piwnica-Worms (Washington University) and maintained in DMEM supplemented with 10% FBS, 0.1% penicillin/streptomycin, and 1 mg/mL G418 (Washington University Tissue Culture Support Center). Human dermal microvascular endothelial cells (HMVEC) were purchased from Lonza and maintained in EGM-2MV medium (Lonza) at 37°C and 5% CO_2. 293A cells were purchased from Invitrogen and maintained at 37°C and 5% CO_2 in DMEM supplemented with 10% FBS and 1% penicillin/streptomycin.

siRNA kinome screen

The Human Kinase siRNA library set version 2.0 was provided by Qiagen. Fully annealed duplex siRNAs were suspended in 1X annealing buffer (100 mM KOAc, 30 mM HEPES-KOH, 2 mM MgOAc, pH 7.4) and 0.25 nmol of pooled siRNAs were stored at −80°C until further use. HeLa-Fluc cells were seeded at 1×10^4 cells/well in thirty-six 96-well plates (Costar) and grown overnight at 37°C and 5% CO_2. The next day, each well was transfected with a duplex of siRNAs (50 nM) targeting a specific kinase, and cells were subsequently incubated for 48 h at 37°C. STx1 (1 ng/mL) was added for 24 h, and light levels were determined using the PerkinElmer Envision XCite Multilabel Reader (1 min delay, 1 s integration). Following luminescence readings, 10 µL of Alamar Blue (440 µM resazurin sodium salt stock; Sigma) were added to each well, and plates were incubated for 2 h at 37°C. Alamar Blue levels were detected using the FluoStar OPTIMA spectrophotometer (BMG Labtech).

Each plate contained a positive control and a series of negative controls, as well as a control for transfection efficiency. Positive controls included siRNA against the delta isoform of PKC (PKCδ siRNA, Dharmacon; Supplementary Fig. 1A), whose knock-down has been shown to protect against Shiga toxicity (Torgersen *et al.*, 2007), or pretreatment for 1 h with GCA (10 µM), which has been equally shown to be protective against Shiga toxicity (Saenz *et al.*, 2009). Negative controls included cells containing media alone, transfection reagent alone (DharmaFECT1, Dharmacon), negative control siRNA (Dharmacon), scrambled siRNA (Qiagen), and GFP siRNA (Qiagen). Transfection efficiency was controlled for by transfecting cells with siRNA targeting the luciferase reporter (GL3 siRNA; Dharmacon) and ensuring >75% drop in light levels (Supplementary Fig. 1B). All controls were validated prior to incorporating them in the screen (Supplementary Fig. 2). MK2 duplex siRNA

sequences provided in the Qiagen library were as follows: 5'-
CGCCATCATCGATGACTACAA-3' and 5'-CTACGAGCAGATCAAGATAAA-3'.

Western blotting

Following compound and toxin treatments, cells were lysed in lysis buffer (20 mM Tris-HCl
pH 7.5, 150 mM NaCl, 1 mM Na_2EDTA, 1 mM EGTA, 1% Triton, 2.5 mM sodium
pyrophosphate, 1 mM β-glycerophosphate, 1 mM Na_3VO_4, 1 μg/mL leupeptin, 1X protease
inhibitor cocktail) and resolved on a 4-15% Tris-HCl gel (Biorad) prior to transfer onto
PVDF membranes (Invitrogen). Membranes were probed with corresponding primary
antibodies (1:1000) and anti-rabbit alkaline phosphatase-conjugated secondary antibodies
(Invitrogen). Membranes were washed and developed using the Western Breeze kit protocol
(Invitrogen). For experiments comparing multiple phospho-proteins, membranes were
washed and reprobed with additional antibodies. Where indicated, equal fractions of lysates
from the same experiment were run on separate gels and probed with the corresponding
primary antibodies.

Overexpression of MK2-WT and MK2-DN

Recombinant wild-type MK2 (MK2-WT) and catalytically inactive MK2 (MK2-DN)
adenoviruses were purchased from Cell Biolabs, Inc. and amplified in 293A cells using the
manufacturer's protocol. The pAd-Luc adenoviral construct has been previously reported
and validated (Zhao and Haslam, 2005). Viral stocks were stored at −80°C until further use.
Confluent HeLa cells were transduced for 24 h prior to a 6-h expsoure to STx1 (10 ng/mL).
Lysates were probed by Western blotting with antibodies to MK2, phospho-Hsp27, and β-
actin. For cytokine mRNA measurements, HeLa cells were transduced for 24 h, exposed to
STx1 for 6h, and RNA was harvested using the RNeasy Mini Kit (Qiagen), according to the
manufacturer's protocol.

Quantitative PCR (qPCR)

For cells overexpressing MK2 adenoviral constructs, HeLa cells were transduced for 24 h,
exposed to STx1 for 6h, and RNA was harvested using the RNeasy Mini Kit. For
experiments involving chemical inhibition of MK2, HeLa cells were pretreated with DMSO,
PHA-781089, or SB202190 at the indicated concentrations for 1h at 37°C. Cells were then
left untreated or were exposed to STx1 (100 ng/mL) for 6 h. Cells were washed once with
cold PBS, and RNA was extracted using the RNeasy Mini Kit. cDNA was synthesized in
duplicate from 200 ng of each sample using commercially available primers for GAPDH,
IL-6, and TNFα (Applied Biosystems). For each qPCR run, the calculated threshold cycle
(Ct) was normalized to the threshold cycle of the GAPDH gene amplified from the
corresponding sample. The fold change was calculated using the $2^{-\Delta\Delta Ct}$ method (Livak and
Schmittgen, 2001) and represents the fold change above adenovirally-transduced or
compound-treated cells lacking STx1 treatment.

Statistical analyses

Data were processed and analyzed using GraphPad Prism version 5.00 for Windows
(GraphPad software). Cytokine mRNA levels were compared using the two-tailed Student's
t-test (VassarStats, http://faculty.vassar.edu/lowry/tu.html) for three independent
experiments. Differences were considered significant for $p<0.05$ and highly significant for
$p<0.01$.

Supplementary Material

Refer to Web version on PubMed Central for supplementary material.

Acknowledgments

References

Allen M, Svensson L, Roach M, Hambor J, McNeish J, Gabel CA. Deficiency of the stress kinase p38alpha results in embryonic lethality: characterization of the kinase dependence of stress responses of enzyme-deficient embryonic stem cells. J Exp Med. 2000; 191:859–870. [PubMed: 10704466]

Anderson DR, Hegde S, Reinhard E, Gomez L, Vernier WF, Lee L, et al. Aminocyanopyridine inhibitors of mitogen activated protein kinase-activated protein kinase 2 (MK-2). Bioorg Med Chem Lett. 2005; 15:1587–1590. [PubMed: 15745802]

Anderson DR, Meyers MJ, Vernier WF, Mahoney MW, Kurumbail RG, Caspers N, et al. Pyrrolopyridine inhibitors of mitogen-activated protein kinase-activated protein kinase 2 (MK-2). J Med Chem. 2007; 50:2647–2654. [PubMed: 17480064]

Carballo E, Cao H, Lai WS, Kennington EA, Campbell D, Blackshear PJ. Decreased sensitivity of tristetraprolin-deficient cells to p38 inhibitors suggests the involvement of tristetraprolin in the p38 signaling pathway. J Biol Chem. 2001; 276:42580–42587. [PubMed: 11546803]

Carey KL, Westwood NJ, Mitchison TJ, Ward GE. A small-molecule approach to studying invasive mechanisms of Toxoplasma gondii. Proceedings of the National Academy of Sciences of the United States of America. 2004; 101:7433–7438. [PubMed: 15123807]

Cherla RP, Lee SY, Mees PL, Tesh VL. Shiga toxin 1-induced cytokine production is mediated by MAP kinase pathways and translation initiation factor eIF4E in the macrophage-like THP-1 cell line. J Leukoc Biol. 2006; 79:397–407. [PubMed: 16301326]

Deng Q, Barbieri JT. Molecular mechanisms of the cytotoxicity of ADP-ribosylating toxins. Annu Rev Microbiol. 2008; 62:271–288. [PubMed: 18785839]

Dominguez C, Powers DA, Tamayo N. p38 MAP kinase inhibitors: many are made, but few are chosen. Curr Opin Drug Discov Devel. 2005; 8:421–430.

Endo Y, Tsurugi K. Mechanism of action of ricin and related toxic lectins on eukaryotic ribosomes. Nucleic Acids Symp Ser. 1986:187–190. [PubMed: 3562265]

Falguieres T, Mallard F, Baron C, Hanau D, Lingwood C, Goud B, et al. Targeting of Shiga toxin B-subunit to retrograde transport route in association with detergent-resistant membranes. Molecular Biology of the Cell. 2001; 12:2453–2468. [PubMed: 11514628]

Falnes PO, Sandvig K. Penetration of protein toxins into cells. Current Opinion in Cell Biology. 2000; 12:407–413. [PubMed: 10873820]

Foster GH, Tesh VL. Shiga toxin 1-induced activation of c-Jun NH(2)-terminal kinase and p38 in the human monocytic cell line THP-1: possible involvement in the production of TNF-alpha. J Leukoc Biol. 2002; 71:107–114. [PubMed: 11781386]

Gaestel M. MAPKAP kinases - MKs - two's company, three's a crowd. Nat Rev Mol Cell Biol. 2006; 7:120–130. [PubMed: 16421520]

Gaestel M, Kotlyarov A, Kracht M. Targeting innate immunity protein kinase signalling in inflammation. Nat Rev Drug Discov. 2009; 8:480–499. [PubMed: 19483709]

Gorska MM, Liang Q, Stafford SJ, Goplen N, Dharajiya N, Guo L, et al. MK2 controls the level of negative feedback in the NF-kappaB pathway and is essential for vascular permeability and airway inflammation. J Exp Med. 2007; 204:1637–1652. [PubMed: 17576778]

Griffin PM, Tauxe RV. The epidemiology of infections caused by Escherichia coli O157:H7, other enterohemorrhagic E. coli, and the associated hemolytic uremic syndrome. Epidemiol Rev. 1991; 13:60–98. [PubMed: 1765120]

Gross S, Piwnica-Worms D. Real-time imaging of ligand-induced IKK activation in intact cells and in living mice. Nat Methods. 2005; 2:607–614. [PubMed: 16094386]

Guessous F, Marcinkiewicz M, Polanowska-Grabowska R, Kongkhum S, Heatherly D, Obrig T, Gear AR. Shiga toxin 2 and lipopolysaccharide induce human microvascular endothelial cells to release chemokines and factors that stimulate platelet function. Infect Immun. 2005; 73:8306–8316. [PubMed: 16299328]

Harel Y, Silva M, Giroir B, Weinberg A, Cleary TB, Beutler B. A reporter transgene indicates renal-specific induction of tumor necrosis factor (TNF) by shiga-like toxin. Possible involvement of TNF in hemolytic uremic syndrome. J Clin Invest. 1993; 92:2110–2116. [PubMed: 8227326]

Henry JR, Rupert KC, Dodd JH, Turchi IJ, Wadsworth SA, Cavender DE, et al. Potent inhibitors of the MAP kinase p38. Bioorg Med Chem Lett. 1998; 8:3335–3340. [PubMed: 9873730]

Hung DT, Shakhnovich EA, Pierson E, Mekalanos JJ. Small-molecule inhibitor of Vibrio cholerae virulence and intestinal colonization. Science. 2005; 310:670–674. [PubMed: 16223984]

Iordanov MS, Pribnow D, Magun JL, Dinh TH, Pearson JA, Chen SL, Magun BE. Ribotoxic stress response: activation of the stress-activated protein kinase JNK1 by inhibitors of the peptidyl transferase reaction and by sequence-specific RNA damage to the alpha-sarcin/ricin loop in the 28S rRNA. Mol Cell Biol. 1997; 17:3373–3381. [PubMed: 9154836]

Janes KA, Reinhardt HC, Yaffe MB. Cytokine-induced signaling networks prioritize dynamic range over signal strength. Cell. 2008; 135:343–354. [PubMed: 18957207]

Karmali MA. Infection by verocytotoxin-producing Escherichia coli. Clinical Microbiology Reviews. 1989; 2:15–38. [PubMed: 2644022]

Katagiri YU, Mori T, Nakajima H, Katagiri C, Taguchi T, Takeda T, et al. Activation of Src family kinase yes induced by Shiga toxin binding to globotriaosyl ceramide (Gb3/CD77) in low density, detergent-insoluble microdomains. J Biol Chem. 1999; 274:35278–35282. [PubMed: 10575015]

Kaye SA, Louise CB, Boyd B, Lingwood CA, Obrig TG. Shiga toxin-associated hemolytic uremic syndrome: interleukin-1 beta enhancement of Shiga toxin cytotoxicity toward human vascular endothelial cells in vitro. Infect Immun. 1993; 61:3886–3891. [PubMed: 8359910]

Kotlyarov A, Neininger A, Schubert C, Eckert R, Birchmeier C, Volk HD, Gaestel M. MAPKAP kinase 2 is essential for LPS-induced TNF-alpha biosynthesis. Nat Cell Biol. 1999; 1:94–97. [PubMed: 10559880]

Lauvrak SU, Walchli S, Iversen TG, Slagsvold HH, Torgersen ML, Spilsberg B, Sandvig K. Shiga toxin regulates its entry in a Syk-dependent manner. Mol Biol Cell. 2006; 17:1096–1109. [PubMed: 16371508]

Lindgren SW, Samuel JE, Schmitt CK, O'Brien AD. The specific activities of Shiga-like toxin type II (SLT-II) and SLT-II-related toxins of enterohemorrhagic Escherichia coli differ when measured by Vero cell cytotoxicity but not by mouse lethality. Infect Immun. 1994; 62:623–631. [PubMed: 8300218]

Livak KJ, Schmittgen TD. Analysis of relative gene expression data using real-time quantitative PCR and the 2(-Delta Delta C(T)) Method. Methods. 2001; 25:402–408. [PubMed: 11846609]

Louise CB, Obrig TG. Shiga toxin-associated hemolytic uremic syndrome: combined cytotoxic effects of shiga toxin and lipopolysaccharide (endotoxin) on human vascular endothelial cells in vitro. Infect Immun. 1992; 60:1536–1543. [PubMed: 1548077]

Mahtani KR, Brook M, Dean JL, Sully G, Saklatvala J, Clark AR. Mitogen-activated protein kinase p38 controls the expression and posttranslational modification of tristetraprolin, a regulator of tumor necrosis factor alpha mRNA stability. Mol Cell Biol. 2001; 21:6461–6469. [PubMed: 11533235]

Morigi M, Galbusera M, Binda E, Imberti B, Gastoldi S, Remuzzi A, et al. Verotoxin-1-induced up-regulation of adhesive molecules renders microvascular endothelial cells thrombogenic at high shear stress. Blood. 2001; 98:1828–1835. [PubMed: 11535517]

Mudgett JS, Ding J, Guh-Siesel L, Chartrain NA, Yang L, Gopal S, Shen MM. Essential role for p38alpha mitogen-activated protein kinase in placental angiogenesis. Proc Natl Acad Sci U S A. 2000; 97:10454–10459. [PubMed: 10973481]

Neininger A, Kontoyiannis D, Kotlyarov A, Winzen R, Eckert R, Volk HD, et al. MK2 targets AU-rich elements and regulates biosynthesis of tumor necrosis factor and interleukin-6 independently at different post-transcriptional levels. J Biol Chem. 2002; 277:3065–3068. [PubMed: 11741878]

Obrig TG, Moran TP, Brown JE. The mode of action of Shiga toxin on peptide elongation of eukaryotic protein synthesis. Biochem J. 1987; 244:287–294. [PubMed: 3663122]

Obrig TG, Louise CB, Lingwood CA, Boyd B, Barley-Maloney L, Daniel TO. Endothelial heterogeneity in Shiga toxin receptors and responses. J Biol Chem. 1993; 268:15484–15488. [PubMed: 8340376]

Obrig TG, Del Vecchio PJ, Brown JE, Moran TP, Rowland BM, Judge TK, Rothman SW. Direct cytotoxic action of Shiga toxin on human vascular endothelial cells. Infect Immun. 1988; 56:2373–2378. [PubMed: 3044997]

Ono K, Han J. The p38 signal transduction pathway: activation and function. Cell Signal. 2000; 12:1–13. [PubMed: 10676842]

Ostroff SM, Tarr PI, Neill MA, Lewis JH, Hargrett-Bean N, Kobayashi JM. Toxin genotypes and plasmid profiles as determinants of systemic sequelae in Escherichia coli O157:H7 infections. J Infect Dis. 1989; 160:994–998. [PubMed: 2685131]

Paros M, Tarr PI, Kim H, Besser TE, Hancock DD. A comparison of human and bovine Escherichia coli O157:H7 isolates by toxin genotype, plasmid profile, and bacteriophage lambda-restriction fragment length polymorphism profile. J Infect Dis. 1993; 168:1300–1303. [PubMed: 8053998]

Pestka S. Inhibitors of ribosome functions. Annu Rev Microbiol. 1971; 25:487–562. [PubMed: 4949424]

Pijpers AH, van Setten PA, van den Heuvel LP, Assmann KJ, Dijkman HB, Pennings AH, et al. Verocytotoxin-induced apoptosis of human microvascular endothelial cells. J Am Soc Nephrol. 2001; 12:767–778. [PubMed: 11274238]

Proulx F, Seidman EG, Karpman D. Pathogenesis of Shiga toxin-associated hemolytic uremic syndrome. Pediatr Res. 2001; 50:163–171. [PubMed: 11477199]

Ramegowda B, Tesh VL. Differentiation-associated toxin receptor modulation, cytokine production, and sensitivity to Shiga-like toxins in human monocytes and monocytic cell lines. Infect Immun. 1996; 64:1173–1180. [PubMed: 8606075]

Reisbig R, Olsnes S, Eiklid K. The cytotoxic activity of Shigella toxin. Evidence for catalytic inactivation of the 60 S ribosomal subunit. J Biol Chem. 1981; 256:8739–8744. [PubMed: 6894922]

Saenz JB, Doggett TA, Haslam DB. Identification and characterization of small molecules that inhibit intracellular toxin transport. Infect Immun. 2007; 75:4552–4561. [PubMed: 17576758]

Saenz JB, Sun WJ, Chang JW, Li J, Bursulaya B, Gray NS, Haslam DB. Golgicide A reveals essential roles for GBF1 in Golgi assembly and function. Nat Chem Biol. 2009

Samuel JE, Perera LP, Ward S, O'Brien AD, Ginsburg V, Krivan HC. Comparison of the glycolipid receptor specificities of Shiga-like toxin type II and Shiga-like toxin type II variants. Infect Immun. 1990; 58:611–618. [PubMed: 2155181]

Scotland SM, Willshaw GA, Smith HR, Rowe B. Properties of strains of Escherichia coli belonging to serogroup O157 with special reference to production of Vero cytotoxins VT1 and VT2. Epidemiol Infect. 1987; 99:613–624. [PubMed: 3322851]

Simpson JC, Roberts LM, Romisch K, Davey J, Wolf DH, Lord JM. Ricin A chain utilises the endoplasmic reticulum-associated protein degradation pathway to enter the cytosol of yeast. FEBS Letters. 1999; 459:80–84. [PubMed: 10508921]

Skanland SS, Walchli S, Sandvig K. beta-arrestins attenuate p38 mediated endosome to Golgi transport. Cell Microbiol. 2009

Smith WE, Kane AV, Campbell ST, Acheson DW, Cochran BH, Thorpe CM. Shiga toxin 1 triggers a ribotoxic stress response leading to p38 and JNK activation and induction of apoptosis in intestinal epithelial cells. Infect Immun. 2003; 71:1497–1504. [PubMed: 12595468]

Somwar R, Koterski S, Sweeney G, Sciotti R, Djuric S, Berg C, et al. A dominant-negative p38 MAPK mutant and novel selective inhibitors of p38 MAPK reduce insulin-stimulated glucose uptake in 3T3-L1 adipocytes without affecting GLUT4 translocation. J Biol Chem. 2002; 277:50386–50395. [PubMed: 12393894]

Stoecklin G, Stubbs T, Kedersha N, Wax S, Rigby WF, Blackwell TK, Anderson P. MK2-induced tristetraprolin:14-3-3 complexes prevent stress granule association and ARE-mRNA decay. Embo J. 2004; 23:1313–1324. [PubMed: 15014438]

Stone MK, Kolling GL, Lindner MH, Obrig TG. p38 mitogen-activated protein kinase mediates lipopolysaccharide and tumor necrosis factor alpha induction of shiga toxin 2 sensitivity in human umbilical vein endothelial cells. Infect Immun. 2008; 76:1115–1121. [PubMed: 18086809]

Stricklett PK, Hughes AK, Kohan DE. Inhibition of p38 mitogen-activated protein kinase ameliorates cytokine up-regulated shigatoxin-1 toxicity in human brain microvascular endothelial cells. J Infect Dis. 2005; 191:461–471. [PubMed: 15633106]

Sun L, Stoecklin G, Van Way S, Hinkovska-Galcheva V, Guo RF, Anderson P, Shanley TP. Tristetraprolin (TTP)-14-3-3 complex formation protects TTP from dephosphorylation by protein phosphatase 2a and stabilizes tumor necrosis factor-alpha mRNA. J Biol Chem. 2007; 282:3766–3777. [PubMed: 17170118]

Takenouchi H, Kiyokawa N, Taguchi T, Matsui J, Katagiri YU, Okita H, et al. Shiga toxin binding to globotriaosyl ceramide induces intracellular signals that mediate cytoskeleton remodeling in human renal carcinoma-derived cells. J Cell Sci. 2004; 117:3911–3922. [PubMed: 15265987]

Tamura K, Sudo T, Senftleben U, Dadak AM, Johnson R, Karin M. Requirement for p38alpha in erythropoietin expression: a role for stress kinases in erythropoiesis. Cell. 2000; 102:221–231. [PubMed: 10943842]

Tarr PI, Gordon CA, Chandler WL. Shiga-toxin-producing Escherichia coli and haemolytic uraemic syndrome. Lancet. 2005; 365:1073–1086. [PubMed: 15781103]

Te Loo DM, Monnens L, van der Velden T, Karmali M, van den Heuvel L, van Hinsbergh V. Shiga toxin-1 affects nitric oxide production by human glomerular endothelial and mesangial cells. Pediatr Nephrol. 2006; 21:1815–1823. [PubMed: 16944213]

Tesh VL, Burris JA, Owens JW, Gordon VM, Wadolkowski EA, O'Brien AD, Samuel JE. Comparison of the relative toxicities of Shiga-like toxins type I and type II for mice. Infect Immun. 1993; 61:3392–3402. [PubMed: 8335369]

Torgersen ML, Walchli S, Grimmer S, Skanland SS, Sandvig K. Protein kinase Cdelta is activated by Shiga toxin and regulates its transport. J Biol Chem. 2007; 282:16317–16328. [PubMed: 17403690]

van de Kar NC, Monnens LA, Karmali MA, van Hinsbergh VW. Tumor necrosis factor and interleukin-1 induce expression of the verocytotoxin receptor globotriaosylceramide on human endothelial cells: implications for the pathogenesis of the hemolytic uremic syndrome. Blood. 1992; 80:2755–2764. [PubMed: 1333300]

van Setten PA, van Hinsbergh VW, van der Velden TJ, van de Kar NC, Vermeer M, Mahan JD, et al. Effects of TNF alpha on verocytotoxin cytotoxicity in purified human glomerular microvascular endothelial cells. Kidney Int. 1997; 51:1245–1256. [PubMed: 9083293]

Walchli S, Skanland SS, Gregers TF, Lauvrak SU, Torgersen ML, Ying M, et al. The Mitogen-activated protein kinase p38 links Shiga Toxin-dependent signaling and trafficking. Mol Biol Cell. 2008; 19:95–104. [PubMed: 17959827]

Wang X, Mader MM, Toth JE, Yu X, Jin N, Campbell RM, et al. Complete inhibition of anisomycin and UV radiation but not cytokine induced JNK and p38 activation by an aryl-substituted dihydropyrrolopyrazole quinoline and mixed lineage kinase 7 small interfering RNA. J Biol Chem. 2005; 280:19298–19305. [PubMed: 15737997]

Wilcke M, Johannes L, Galli T, Mayau V, Goud B, Salamero J. Rab11 regulates the compartmentalization of early endosomes required for efficient transport from early endosomes to the trans-golgi network. Journal of Cell Biology. 2000; 151:1207–1220. [PubMed: 11121436]

Yates SP, Merrill AR. Elucidation of eukaryotic elongation factor-2 contact sites within the catalytic domain of Pseudomonas aeruginosa exotoxin A. Biochem J. 2004; 379:563–572. [PubMed: 14733615]

Yu M, Haslam DB. Shiga toxin is transported from the endoplasmic reticulum following interaction with the luminal chaperone HEDJ/ERdj3. Infection & Immunity. 2005; 73:2524–2532. [PubMed: 15784599]

Yu M, Haslam RH, Haslam DB. HEDJ, an Hsp40 co-chaperone localized to the endoplasmic reticulum of human cells. Journal of Biological Chemistry. 2000; 275:24984–24992. [PubMed: 10827079]

Zarubin T, Han J. Activation and signaling of the p38 MAP kinase pathway. Cell Res. 2005; 15:11–18. [PubMed: 15686620]

Zhao L, Haslam DB. A quantitative and highly sensitive luciferase-based assay for bacterial toxins that inhibit protein synthesis. J Med Microbiol. 2005; 54:1023–1030. [PubMed: 16192432]
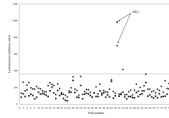
Fig. 1.
Knock-down of MK2 protects against Shiga toxicity. A siRNA screen of 646 human kinase and kinase-associated genes was adapted to a 96-well format (see Experimental procedures). Shown are two representative plates, run in duplicate (circles and squares), demonstrating light levels of 80 different kinase siRNAs after a 24-h treatment with STx1 (1 ng/mL). Well number represents each well of HeLa-Fluc cells transfected with 50 nM siRNA targeting a specific kinase, and corresponding light levels are shown on the y-axis. Control wells have been excluded (see Supplementary Fig. 2). A hit was considered any knock-down that maintained luminescence at least 3 standard deviations above STx1-treated controls (dotted line). Knock-down of MK2 (siRNA sequence provided in Experimental Procedures) conferred the highest protection against Shiga toxicity. Mean and standard deviations for each set of duplicate plates were determined by GraphPad Prism. MK2, mitogen-activated protein kinase-activated protein kinase 2.
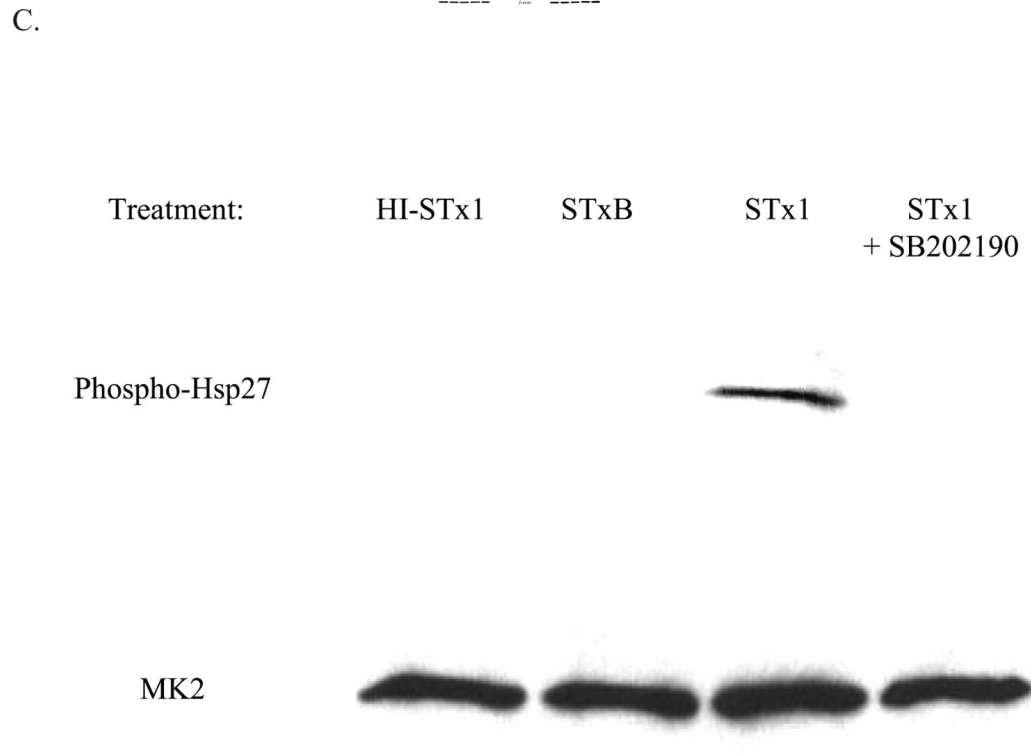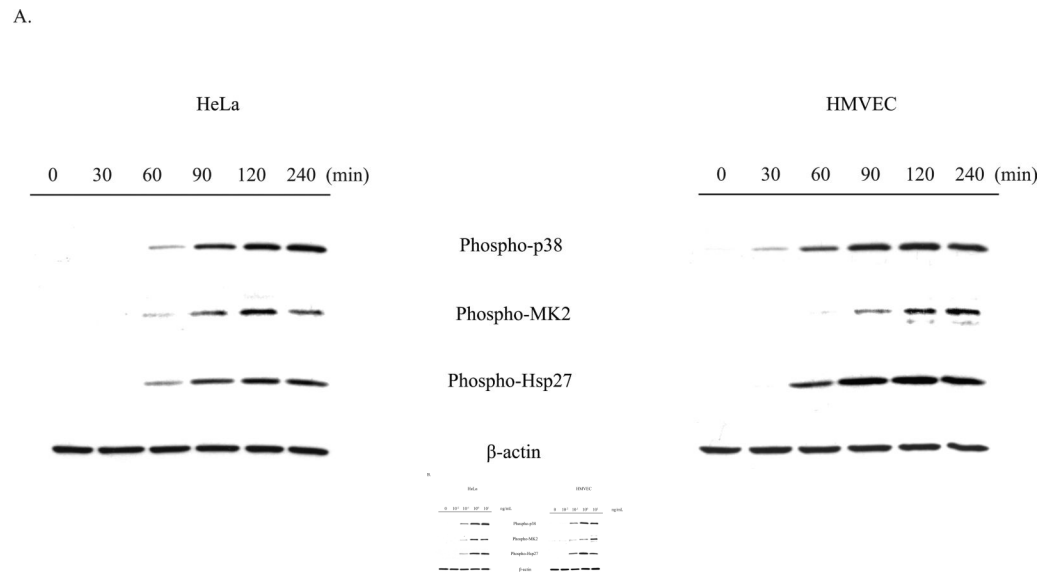
A.

HeLa

| 0 | 30 | 60 | 90 | 120 | 240 | (min) |

HMVEC

| 0 | 30 | 60 | 90 | 120 | 240 | (min) |

Phospho-p38

Phospho-MK2

Phospho-Hsp27

β-actin

C.

Treatment: HI-STx1   STxB   STx1   STx1
                                              + SB202190

Phospho-Hsp27

MK2

Fig. 2.
STx1 specifically induces activation of the p38-MK2 pathway in both HeLa and HMVEC in time- and dose-dependent manners.
A. HeLa cells (left) or HMVEC (right) were treated with no toxin or STx1 (10 ng/mL) for the indicated times, and lysates were probed with the indicated antibodies. Activation of the p38-MK2 pathway is observed by 60 min following exposure to STx1, while stimulation of this pathway in HMVEC can be seen as early as 30 min.
B. HeLa cells (left) or HMVEC (right) were treated with either no toxin or increasing STx1 concentrations for 2 h. Lysates were probed as in (A). For both cell lines, as little as 0.1 ng/

mL STx1 was able to activate the p38-MK2 pathway. For (A) and (B), actin staining served as a loading control.

C. HeLa cells were pretreated with DMSO (0.5% v/v) or the p38 inhibitor SB202190 (10 μM) for 1 h prior to a 30-min exposure to STx1 (100 ng/mL). Equal fractions of lysates were probed with the indicated antibodies, with MK2 serving as a loading control. Inhibition of p38 eliminates STx1-induced MK2 activation. In addition, treatment with 100 ng/mL heat-inactivated STx1 (HI-STx1) or the STxB subunit (100 ng/mL) did not activate MK2. Heat inactivation of STx1 involved incubating the toxin for 12 h at 95°C.
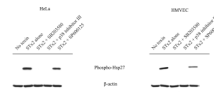
Fig. 3.
STx-induced MK2 activation is p38-specific. HeLa cells (left) or HMVEC (right) were pretreated with the indicated compounds 30 min prior to a 2-h exposure to STx2 (10 ng/mL). Lysates were probed with the indicated antibodies. Two distinct p38 inhibitors, SB203580 (2.65 μM) and the p38 inhibitor III (0.5 μM), prevented STx2-mediated Hsp27 phosphorylation, while the JNK inhibitor SP600125 (25 μM) showed no effect, similar to STx2-treated cells treated lacking compound treatment ("STx2 alone"). "No toxin" refers to cells lacking compound and toxin treatment. β-actin staining served as a loading control.

A.
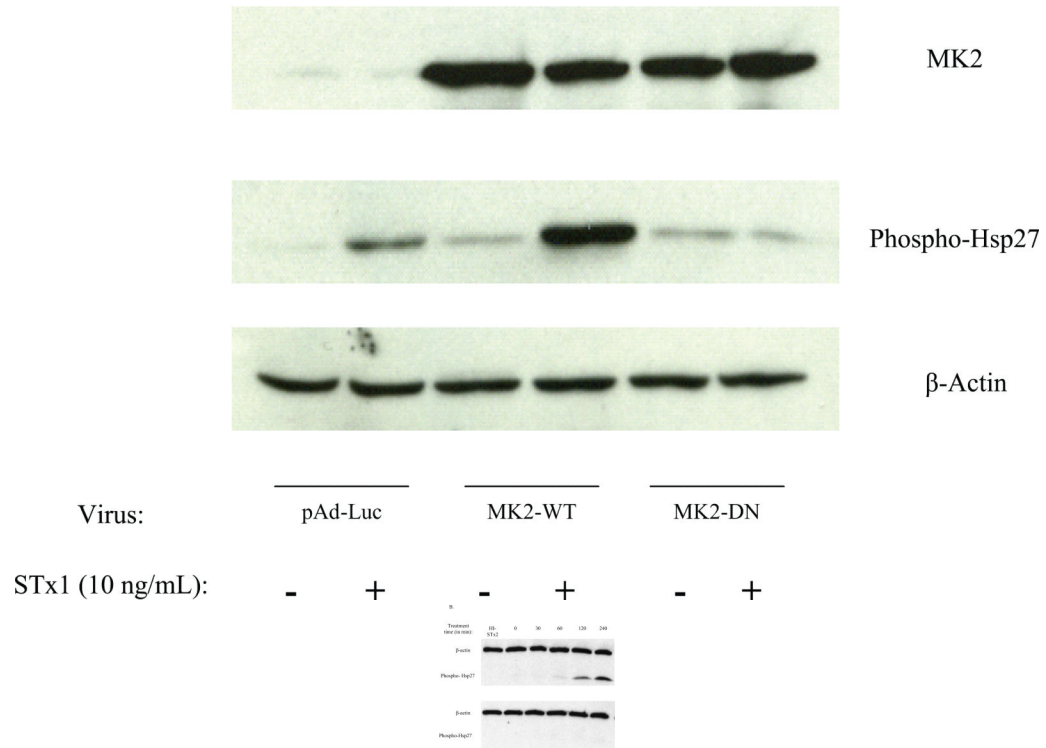
Fig. 4.
STx activation of the p38-MK2 pathway is dependent on MK2 activity.
A. Overexpression of catalytically inactive MK2 (MK2-DN) eliminates STx1-induced Hsp27 phosphorylation. HeLa cells were transduced with adenoviral constructs expressing luciferase (pAd-Luc), wild-type MK2 (MK2-WT), or catalytically inactive MK2 (MK2-DN; see Methods). Cells were then exposed to STx1 (10 ng/mL) for 6 h, and equal fractions of lysates were probed with the indicated antibodies.
B. HMVEC were pretreated with DMSO (0.5% v/v; top) or the MK2 inhibitor PHA-781089 (20 μM; bottom) for 1 h prior to exposure to STx2 (1 ng/mL) for the indicated times. Lysates were probed with the indicated antibodies. Chemical inhibition of MK2 prevents STx-induced Hsp27 phosphorylation. HI-STx2, heat-inactivated STx2 (1 ng/mL). For (A) and (B), actin staining served as a loading control.

B.

None   STx1 STx2 Ricin   DT   PE   Puro CHX

Phospho-p38

Phospho-Hsp27

β-actin
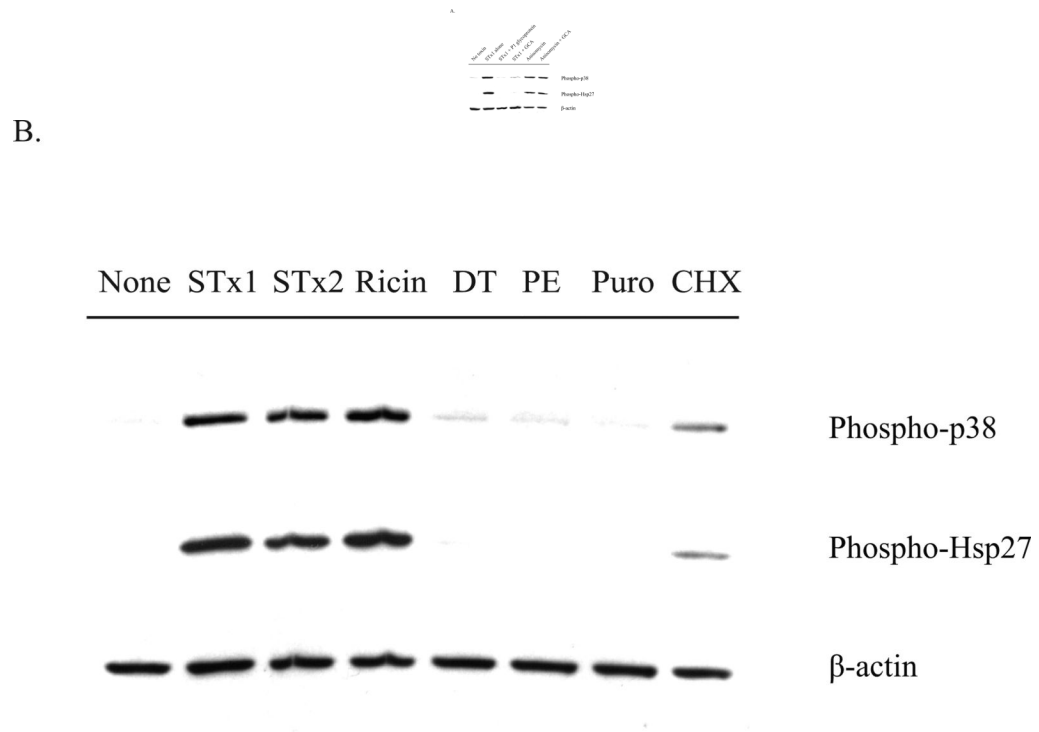
Fig. 5.
Activation of the p38-MK2 pathway by STx depends on toxin adherence and intracellular trafficking and appears to be part of a ribotoxic stress response.

A. HMVEC were pretreated with DMSO (0.5% v/v), GCA (10 μM), or P1 glycoprotein (1 μg/mL) for 30 min prior to exposure to STx1 (10 ng/mL) or media alone ("No Toxin"). Cells were allowed to internalize toxin for 2 h at 37°C prior to lysis and probing with the indicated antibodies. Pretreatment with the P1 glycoprotein inhibited STx1-mediated phosphorylation of p38 and Hsp27, and GCA treatment similarly blocked activation of the p38-MK2 pathway compared to DMSO-treated cells ("Toxin alone"). Pretreatment with GCA, however, had no effect on activation of this pathway following a 2-h exposure to anisomycin (10 ng/mL).

B. HMVEC were exposed to various translational inhibitors for 2 h, and the phosphorylation status of p38 and Hsp27 was assessed by Western blotting. Only inhibitors that are known to cause direct damage to the ribosome (STx1, STx2, and ricin) induced p38 and Hsp27 phosphorylation, while translational inhibitors acting through different mechanisms (DT, PE, Puro, CHX) showed little to no activation. "None" refers to cells lacking compound and toxin treatment. STx1, Shiga toxin 1 (10 ng/mL); STx2, Shiga toxin 2 (10 ng/mL); GCA, Golgicide A; DT, diphtheria toxin (1 μg/mL); PE, *Pseudomonas* exotoxin A (1 μg/mL); Puro, puromycin (10 μg/mL); CHX, cycloheximide (100 μg/mL). For both (A) and (B), actin staining served as a loading control.

A.

B.

C.

D.
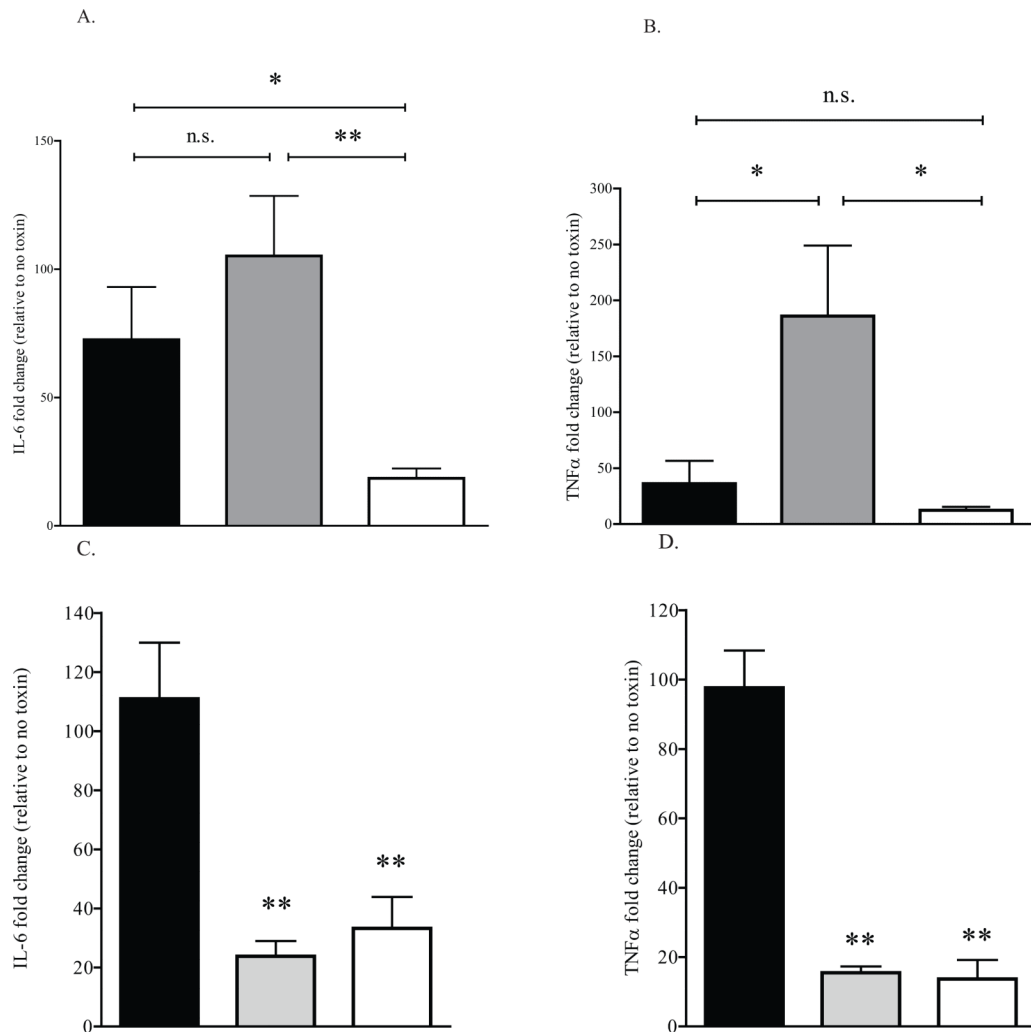
Fig. 6.
MK2 inhibition reduces the STx1-induced inflammatory response.
A. HeLa cells were transduced with a control adenoviral construct (pAd-Luc; black bars), a construct expressing wild-type MK2 (MK2-WT; gray bars), or a construct expressing a catalytically inactive MK2 (MK2-DN; white bars) for 24 h prior to treating with STx1 (10 ng/mL) for 6 h. The levels of IL-6 and TNFα mRNA were determined by qPCR and are expressed as a fold change above mRNA levels in transduced cells lacking STx1 (see Experimental Procedures). Data points represent duplicate data from three independent experiments (mean ±S.D.). Sample means were compared using a two-tailed Student's t-test for independent samples.
B. HeLa cells were pretreated with DMSO (0.5% v/v; black bars), the MK2 inhibitor PHA-781089 (20 μM; gray bars), or the p38 inhibitor SB202190 (10 μM; white bars) for 1 h prior to a 6-h exposure to STx1 (100 ng/mL). The levels of IL-6 and TNFα mRNA were determined by qPCR and are expressed as a fold change above mRNA levels in compound-treated cells in the absence of STx1. Data points represent duplicate data from three independent experiments (mean ±S.D.). Sample means were compared as in (A). n.s. denotes no significant change, * significant change (p<0.05), ** highly significant change (p<0.01).